The protease SENP2 controls hepatic gluconeogenesis by regulating the SUMOylation of the fuel sensor AMPKα

Received for publication, November 23, 2021, and in revised form, December 18, 2021 Published, Papers in Press, December 28, 2021,
https://doi.org/10.1016/j.jbc.2021.101544

Xin Dou[‡], Wei-Yu Zhou[‡], Meng Ding, Yin-Jun Ma, Qi-Qi Yang, Shu-Wen Qian, Yan Tang, Qi-Qun Tang[*], and Yang Liu[*]

From the Key Laboratory of Metabolism and Molecular Medicine of the Ministry of Education, Department of Biochemistry and Molecular Biology of School of Basic Medical Sciences, and Department of Endocrinology and Metabolism of Zhongshan Hospital, and Department of Clinical Laboratory, Shanghai Pudong Hospital, Fudan University, Shanghai, China

Edited by Eric Fearon

Uncontrolled gluconeogenesis results in elevated hepatic glucose production in type 2 diabetes (T2D). The small ubiquitin-related modifier (SUMO)-specific protease 2 (SENP2) is known to catalyze deSUMOylation of target proteins, with broad effects on cell growth, signal transduction, and developmental processes. However, the role of SENP2 in hepatic gluconeogenesis and the occurrence of T2D remain unknown. Herein, we established SENP2 hepatic knockout mice and found that SENP2 deficiency could protect against high-fat diet–induced hyperglycemia. Pyruvate- or glucagon-induced elevation in blood glucose was attenuated by disruption of SENP2 expression, whereas overexpression of SENP2 in the liver facilitated high-fat diet–induced hyperglycemia. Using an *in vitro* assay, we showed that SENP2 regulated hepatic glucose production. Mechanistically, the effects of SENP2 on gluconeogenesis were found to be mediated by the cellular fuel sensor kinase, 5′-AMP-activated protein kinase alpha (AMPKα), which is a negative regulator of gluconeogenesis. SENP2 interacted with and deSUMOylated AMPKα, thereby promoting its ubiquitination and reducing its protein stability. Inhibition of AMPKα kinase activity dramatically reversed impaired hepatic gluconeogenesis and reduced blood glucose levels in SENP2-deficient mice. Our study highlights the novel role of hepatic SENP2 in regulating gluconeogenesis and furthers our understanding of the pathogenesis of T2D.

Hepatic gluconeogenesis, an essential component of glucose production in healthy individuals, is primarily responsible for maintaining euglycemia during nutrient deprivation (1, 2). During fasting, triglycerides in adipose tissue are hydrolyzed to glycerol and nonesterified fatty acids (3). The released glycerol and lactate predominantly from the muscle are used as the primary precursors for hepatic gluconeogenesis (4). Hepatic glucose output is critical for systemic glucose metabolic homeostasis. In the fasted state, hepatic gluconeogenesis is activated to maintain normal blood glucose levels, ensuring energy demand for glucose-dependent tissues such as the brain. However, uncontrolled hepatic gluconeogenesis is recognized as one of the main contributing factors to hyperglycemia and diabetes. Hepatic gluconeogenesis is tightly regulated by several hormones. For example, it is activated by glucagon and adrenal hormone glucocorticoids and repressed by insulin. In the diabetic state, the liver becomes resistant to insulin and overactivation of hepatic glucose production occurs, leading to uncontrolled blood glucose levels, which are a hallmark of type 2 diabetes (T2D) (5, 6). Several antidiabetic drugs, such as metformin, target hepatic gluconeogenesis and have hypoglycemic effects. Therefore, studying the regulation of hepatic gluconeogenesis is critical to further the understanding of T2D pathogenesis and offers novel insights into therapeutic strategies for T2D.

Mammalian 5′-AMP-activated protein kinase (AMPK) is regarded as a sensor of rising AMP/ATP and ADP/ATP ratios that emerge under conditions of low cellular energy (7, 8). AMPK is activated by a falling energy state to restore energy balance by switching on ATP-generating catabolic pathways, whereas switching off ATP-consuming anabolic pathways, such as lipogenesis and gluconeogenesis (7). AMPK functions as a heterotrimeric complex comprised of a catalytic (AMPKα) and two regulatory (AMPKβ and AMPKγ) subunits (9). The critical phosphorylation site in AMPK, Thr172, is phosphorylated by the upstream liver kinase B1 (10, 11). In the canonical mechanism of AMPK activation, 5′-AMP binds to the AMPKγ subunit, leading to allosteric activation of Thr172-phosphorylated AMPK, and maintenance of the enhanced Thr172 phosphorylated state (7). AMPK is considered to be an inhibitor of gluconeogenesis, *via* phosphorylation of the cAMP response element–binding protein (CREB) coactivator, transducer of regulated CREB activity 2 (TORC2). Phosphorylated TORC2 is sequestered in the cytoplasm, thereby inhibiting CREB-dependent transcription of peroxisome proliferator–activated receptor γ coactivator 1α and gluconeogenic enzyme genes (12, 13). Thus, identifying factors that regulate the expression or activity of AMPK is crucial for understanding the process of gluconeogenesis and may lead to the development of novel therapeutic strategies for T2D.

Protein post-translational modifications with small ubiquitin-related modifier (SUMO) are highly conserved in

[‡] These authors contributed equally to this work.
[*] For correspondence: Qi-Qun Tang, qqtang@shmu.edu.cn; Yang Liu, yangliuly@fudan.edu.cn.

all eukaryotes (14). SUMOylation is catalyzed by Aos1/Uba2 (an E1-activating enzyme), Ubc9 (an E2-conjugating enzyme), and E3 ligases (15). SUMOylation and its related enzymes are involved in cellular processes, such as DNA replication and repair, signal transduction, and cell differentiation (15). We have previously shown that protein inhibitor of activated signal transducer and activator of transcription-1, the SUMO E3 ligase, controls adipogenesis by promoting the SUMOylation and degradation of CCAAT/enhancer binding protein β (16). Subsequent studies have clarified that protein inhibitor of activated signal transducer and activator of transcription-1 in adipose tissues could activate the insulin signaling pathway, thereby improving insulin sensitivity in T2D mice (17).

SUMOylation is a dynamic and reversible protein modification. SUMO-specific protease 2 (SENP2), a member of the SENP family, is responsible for the catalyzation of deSUMOylation (18). SENP2 is reportedly essential for adipocyte differentiation, including the differentiation of white adipocytes and brown adipocytes (19–21). SENP2 has also been shown to regulate insulin sensitivity in muscle cells (22). We have previously reported that loss of hepatic SENP2 prevents nonalcoholic fatty liver disease development induced by high-fat diet (HFD) (23). These data suggest that SENP2 plays a key role in modulating metabolic balance. However, the roles of SENP2 in hepatic glucose metabolism remain unknown. Here, we established SENP2 hepatic knockout mice and found that liver-specific SENP2 deficiency could protect against HFD-induced hyperglycemia, whereas overexpression of SENP2 in the liver facilitated the development of HFD-induced hyperglycemia. We also showed that SENP2 regulated blood glucose levels predominantly through the modulation of hepatic gluconeogenesis. Mechanistically, AMPKα mediated the effect of SENP2 on gluconeogenesis. SENP2 deSUMOylated AMPKα, thereby affecting its ubiquitination and stability. Downregulation of AMPKα induced hepatic gluconeogenesis and hyperglycemia. Taken together, our study highlights the novel role of hepatic SENP2 in regulating gluconeogenesis and furthers our understanding of the pathogenesis of T2D.

Results

Hepatic deficiency of SENP2 protects against excessive gluconeogenesis induced by HFD

We have previously shown that SENP2 expression was elevated in the liver of mice with T2D (23). To investigate the effect of SENP2 on hepatic glucose metabolism, we generated liver-specific knockout mice (Senp2-LKO) by crossing $SENP2^{Flox/flox}$ mice with Alb-Cre transgenic mice (Fig. S1, *A* and *B*). Quantitative PCR (qPCR) analysis showed that Senp2 was specifically disrupted in the liver tissues from Senp2-LKO mice (Fig. S1*C*). Senp2-LKO mice developed normally and had body weights similar to WT littermates when fed a normal chow diet (NCD; Fig. S2*A*). Under NCD feeding, there were no differences in fasting blood glucose between Senp2-LKO mice and WT mice; whereas random blood glucose of Senp2-LKO mice was decreased as compared with WT (Fig. S2, *B* and *C*). Glucose production induced by pyruvate or glucagon in Senp2-LKO mice was identical to WT mice as indicated by pyruvate tolerance and glucagon tolerance test (Fig. S2, *D* and *E*). We challenged Senp2-LKO mice and their WT littermates with HFD. Food intake of the two groups was comparable (Fig. S3*A*). Both random and fasting blood glucose levels were decreased in Senp2-LKO mice as compared with WT mice under HFD (Fig. 1, *A* and *B*). The pyruvate tolerance test showed that the levels of glucose produced from pyruvate were lower in the Senp2-LKO mice than control mice (Fig. 1*C*). Glucagon tolerance test showed that Senp2-LKO and WT mice showed similar response to glucagon, although loss of hepatic SENP2 significantly inhibited gluconeogenesis (Fig. 1*D*).

We found that Senp2-LKO mice exhibited resistance to HFD-induced obesity and glucose intolerance (Fig. S3, *B* and *C*). To eliminate the effect of body weight difference on gluconeogenesis, we carried out glucagon tolerance test at fourth week of HFD feeding, when there was no difference in body mass, hepatic steatosis, or insulin sensitivity (Fig. S3, *D* and *E*) and found that gluconeogenesis was also downregulated by SENP2 deficiency at early stage of HFD feeding (Fig. S3*F*). In addition, we isolated primary hepatocytes to examine glucose output *in vitro*. Consistently, glucose production, using lactate and pyruvate as the substrates, was downregulated in SENP2-deficient hepatocytes compared with the controls, no matter under dexamethasone treatment or not (Fig. 1*E*).

Overexpression of SENP2 promotes hepatic gluconeogenesis

To validate our findings in Senp2-LKO mice, we generated adeno-associated virus (AAV) harboring the SENP2 coding sequence and overexpressed SENP2 in the liver by injecting the AAV into the tail vein. AAV-GFP was used as the control. qPCR and Western blot analysis showed that SENP2 was successfully overexpressed (Fig. 2, *A* and *B*). SENP2 overexpression had little effect on random and fasting blood glucose levels under NCD (Fig. 2, *C* and *D*) but dramatically promoted gluconeogenesis induced by pyruvate (Fig. 2*E*). When we challenged the mice with HFD, AAV-SENP2 mice exhibited marked upregulation in both random and fasting blood glucose levels as compared with control mice (Fig. 2, *F* and *G*). In addition, the pyruvate tolerance test showed that ectopic expression of SENP2 significantly augmented glucose production (Fig. 2*H*).

SENP2 regulates hepatic expression of pyruvate carboxylase

Having shown that SENP2 regulated gluconeogenesis, we next examined the expression of rate-limiting gluconeogenic enzymes, including pyruvate carboxylase (PCx), phosphoenolpyruvate carboxykinase 1 (PCK1), and glucose-6-phosphatase (G6PC). qPCR analysis revealed that SENP2 deficiency led to decreased *Pcx* in the liver compared with controls, whereas *Pck1* and *G6pc* expression was unaffected (Fig. 3*A*). Consistent with the mRNA data, PCx protein levels

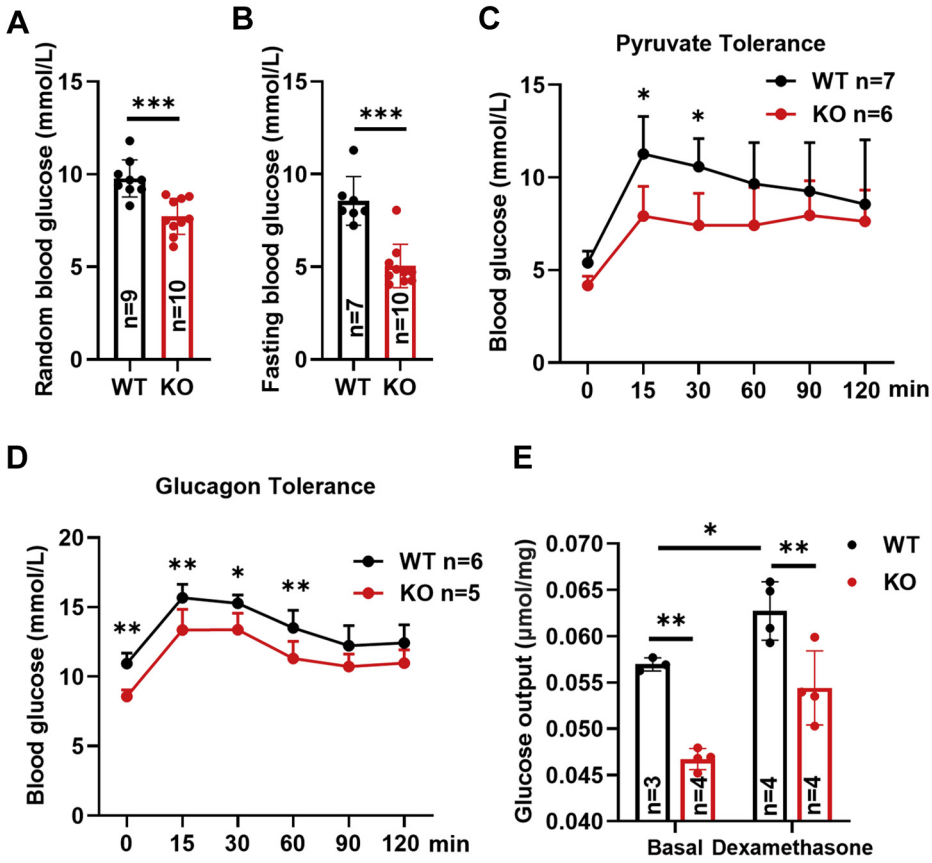

Figure 1. SENP2 deficiency suppressed hepatic gluconeogenesis and decreased blood glucose. *A*, male WT and Senp2-LKO mice were fed with HFD starting at 8 weeks of age. Random blood glucose was measured at 12th week of HFD feeding. *B*, fasting blood glucose was measured after fasting for 16 h at 15th week of HFD feeding. *C*, pyruvate tolerance test was conducted in WT and Senp2-LKO mice at 12th week of HFD feeding. *D*, glucagon tolerance test was conducted in WT and Senp2-LKO mice at 13th week of HFD feeding. *E*, primary hepatocytes were isolated form WT and Senp2-LKO mice and then incubated with glucose substrate solution containing 10 mM sodium lactate, 1 mM sodium pyruvate, with or without 1 μM dexamethasone for 6 h. The content of glucose in cell supernatant was detected and normalized to protein level. Data are presented as mean ± SD. Data in *A* and *B* were analyzed by two-tailed unpaired Student's *t* test; data in *C* and *D* were analyzed by two-way ANOVA with Bonferroni post hoc multiple comparison test. Data in *E* were analyzed using one-way ANOVA with Newman–Keuls test. *$p < 0.05$, **$p < 0.01$, and ***$p < 0.001$. HFD, high-fat diet; LKO, liver-specific knockout mice; SENP2, small ubiquitin–related modifier–specific protease 2.

were also reduced in the liver of Senp2-LKO mice, whereas PCK1 and G6PC were unchanged (Fig. 3, *B* and *C*). Next, we examined gluconeogenic enzymes in isolated primary hepatocytes and found that PCx expression was downregulated in hepatocytes after SENP2 ablation (Fig. 3, *D* and *E*). Consistent with these results, we found that overexpression of SENP2 augmented PCx expression and had little effect on PCK1 and G6PC expression (Fig. 3, *F* and *G*).

SENP2 modulates gluconeogenesis through AMPKα

Having established that SENP2 deficiency attenuates gluconeogenesis and improves HFD-induced hyperglycemia, we next sought to determine the underlying mechanisms. Mammalian AMPK is a sensor of cellular energy. AMPK is activated under situations of increased metabolic demand or in a low cellular energy state and acts to restore energy balance by switching on catabolic pathways such as fatty acid β-oxidation, while switching off anabolic pathways such as lipogenesis and gluconeogenesis (7, 24). Thus, we examined activation of AMPK by measuring the levels of p-AMPKα (Thr172), which is the active catalytic form (24). We found that loss of SENP2 significantly increased p-AMPKα (Thr172) as well as total AMPKα levels in the liver tissue and isolated primary hepatocytes (Fig. 4, *A*–*C*). However, *AMPKα* mRNA levels remained unchanged upon SENP2 deletion (Fig. 4*D*). In addition, phosphorylation of Raptor, the downstream target of AMPK, was increased in SENP2-deficient hepatocytes, indicating augmented activity of AMPKα (Fig. 4*C*).

Since activation of AMPKα was consistent with repressed gluconeogenesis in the liver of Senp2-LKO mice, we next sought to determine whether AMPKα mediated SENP2 function. We isolated primary hepatocytes from WT and Senp2-LKO mice and inhibited AMPK in SENP2-deficient cells using compound C, which is a specific antagonist for AMPK. We found that loss of SENP2 inhibited glucose output compared with the control, whereas compound C significantly restored glucose production in SENP2-ablated cells (Fig. 5*A*). Consistent with these findings, treatment with compound C normalized the decreased expression of PCx in SENP2-ablated cells (Fig. 5*B*). Next, we disrupted AMPKα expression in hepatocytes by siRNA and conducted similar experiments. We found that impaired glucose production in Senp2-LKO cells was reversed by knockdown of AMPKα (Fig. 5*C*). Western blot

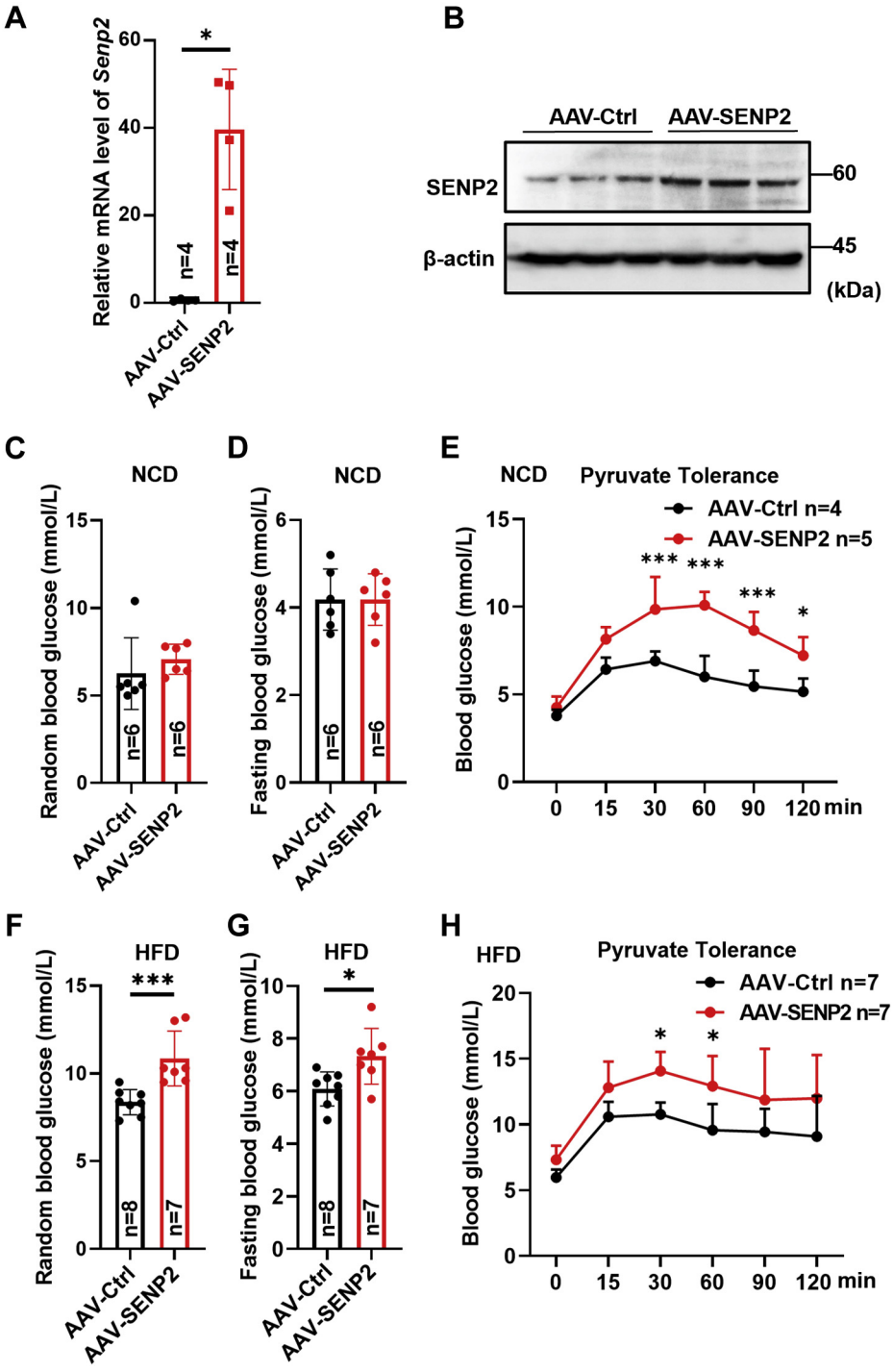

Figure 2. SENP2 overexpression promoted hepatic gluconeogenesis and increased blood glucose. *A* and *B*, SENP2 was overexpressed in liver by injecting AAV serotype 8 into 7-week-old male mice *via* the tail vein. Quantitative PCR and Western blot assay showed the expression of SENP2 in liver. *C*, random blood glucose was measured under NCD feeding. *D*, fasting blood glucose was measured under NCD feeding after fasting for 16 h. *E*, pyruvate tolerance test was conducted in AAV-Ctrl and AAV-SENP2 mice under NCD feeding. *F*, after a week of recovery from AAV injecting, AAV-treated mice were fed with HFD. Random blood glucose was measured at 12th week of HFD feeding. *G*, fasting blood glucose was measured after fasting for 16 h at 13th week of HFD feeding. *H*, pyruvate tolerance test was conducted in AAV-Ctrl and AAV-SENP2 mice at 13th week of HFD feeding. Data are presented as mean ± SD. Data in *A*, *D*, and *G* were analyzed by two-tailed unpaired Student's *t* test. Data in *C* and *F* were analyzed by Mann–Whitney test. Data in *E* and *H* were analyzed by two-way ANOVA with Bonferroni post hoc multiple comparison test. *$p < 0.05$, **$p < 0.01$, and ***$p < 0.001$. AAV, AAV, adeno-associated virus; NCD, normal chow diet; SENP2, small ubiquitin–related modifier–specific protease 2.

analysis showed that AMPKα protein expression was significantly disrupted in Senp2-LKO cells treated with AMPKα siRNA and normalized the expression of PCx, whereas expression of PCK1 and G6PC was unaffected (Fig. 5*D*).

Next, we treated mice with compound C to inhibit AMPK activity *in vivo*. We found that Senp2-LKO mice showed lower random and fasting blood glucose levels than WT mice under HFD conditions (Fig. 5, *E* and *F*), and treatment with

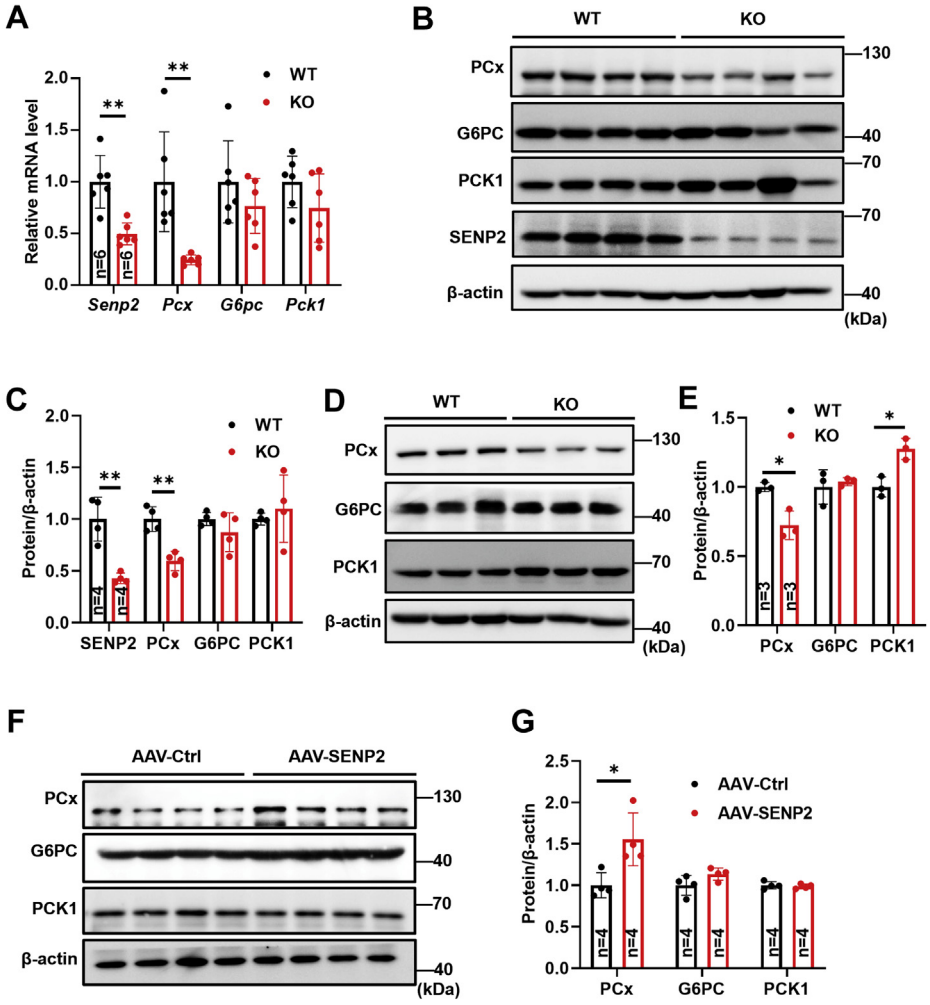

Figure 3. SENP2 regulated PCx expression. *A*, qPCR analysis of *Senp2*, *Pcx*, *G6pc*, and *Pck1* level in the liver of WT and Senp2-LKO mice under HFD. *B* and *C*, protein level of SENP2, PCx, G6PC, and PCK1 in the liver of WT and Senp2-LKO mice under HFD. Level of the bands of these proteins were quantified. *D* and *E*, protein level of PCx, G6PC, and PCK1 in the isolated hepatocytes from WT and Senp2-LKO mice under NCD, with the bands quantified. *F* and *G*, protein level of PCx, G6PC, and PCK1 in the liver of AAV-Ctrl and AAV-SENP2 administration under HFD, with the bands quantified. Data are presented as mean ± SD. Data in *A*, *C*, *E*, and *G* were analyzed by two-tailed unpaired Student's *t* test. *$p < 0.05$ and **$p < 0.01$. G6PC, glucose-6-phosphatase; HFD, high-fat diet; LKO, liver-specific knockout mice; PCK1, phosphoenolpyruvate carboxykinase 1; PCx, pyruvate carboxylase; qPCR, quantitative PCR; SENP2, small ubiquitin–related modifier–specific protease 2.

compound C increased blood glucose levels in Senp2-LKO mice (Fig. 5, *E* and *F*). The glucagon tolerance test demonstrated that compound C treatment restored decreased glucose production in Senp2-LKO mice compared with WT mice (Fig. 5*G*). Consistent with this phenotype, impaired PCx expression in the liver of Senp2-LKO mice was reversed by AMPK inhibition (Fig. 5, *H–J*). Collectively, these results suggest that AMPK mediates the inhibitory effect of SENP2 ablation on gluconeogenesis.

SENP2 regulates the SUMOylation and stability of AMPKα

We next sought to determine the role of SENP2 in the regulation of AMPKα. Although *AMPKα* mRNA levels were unaltered in Senp2-LKO livers, total AMPKα protein levels were increased (Fig. 4, *A–D*), suggesting that SENP2 may regulate AMPKα at the post-transcriptional level. To determine whether SENP2 had a role in directly regulating AMPKα, we performed coimmunoprecipitation assays and found that SENP2 interacted with AMPKα (Fig. 6*A*). Next, we conducted SUMOylation assays in human embryonic kidney 293T (HEK-293T) cells transfected with V5-SUMO2, hemagglutinin (HA)-AMPKα, FLAG-UBC9, and FLAG-SENP2 to determine AMPKα SUMOylation by detection of V5 tag after pull-down of AMPKα. We found that as a SUMO E2-conjugating enzyme, UBC9, increased SUMOylation of AMPKα, whereas SENP2 reversed UBC9-induced SUMOylation of AMPKα (Fig. 6*B*). In addition, we observed that SENP2 also antagonized PIAS4-mediated SUMOylation of AMPKα (Fig. 6*C*). These findings together suggest that SENP2 was responsible for the deSUMOylation of AMPKα.

As SENP2 deficiency increased AMPKα protein level with no effect on its mRNA level, we therefore evaluated the stability of AMPKα protein in control and SENP2-deficient hepatocytes after treatment with cycloheximide, an inhibitor of protein translation. We found that the half-life of AMPKα was markedly increased by SENP2 ablation (Fig. 6*D*). Consistently,

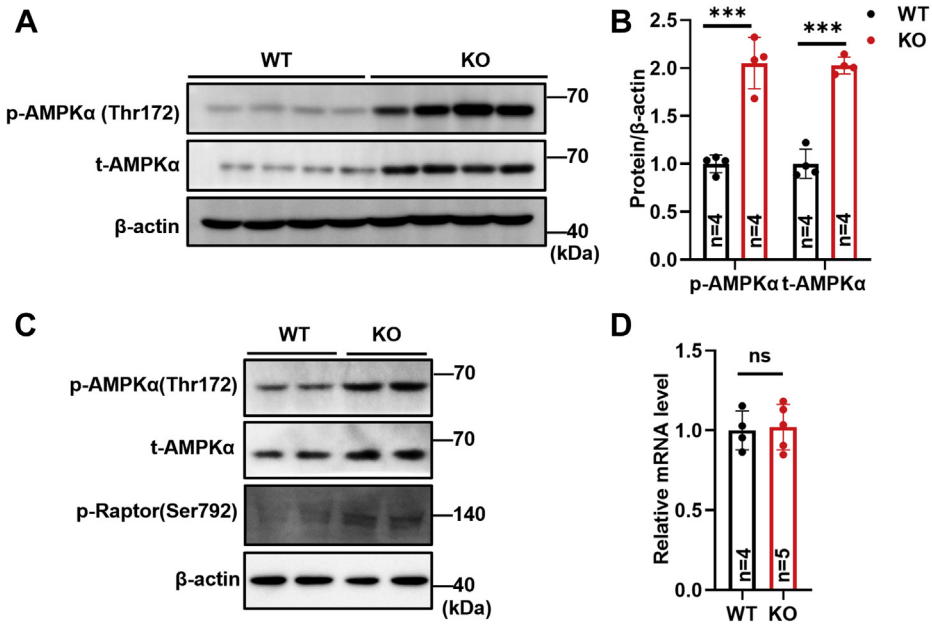

Figure 4. SENP2 deficiency augmented AMPKα level. *A* and *B*, protein level of AMPKα and p-AMPKα in the liver of WT and Senp2-LKO mice, with quantification of these proteins. *C*, protein level of AMPKα, p-AMPKα, and p-Raptor in the primary hepatocytes of WT and Senp2-LKO mice. *D*, qPCR analysis of AMPKα level in the liver of WT and Senp2-LKO mice. Data are presented as mean ± SD. Data in *B* and *D* were analyzed by two-tailed unpaired Student's *t* test. ***$p < 0.001$. AMPK, 5′-AMP-activated protein kinase; LKO, liver-specific knockout mice; qPCR, quantitative PCR; SENP2, small ubiquitin–related modifier–specific protease 2.

SENP2 overexpression reduced AMPKα protein level (Fig. 6*E*). Furthermore, we demonstrated that SENP2 could markedly increase the ubiquitination of AMPKα (Fig. 6*F*). We then sought to detect the stability of deSUMOylated AMPKα to further clarify the relationship between SUMOylation and ubiquitination of AMPKα. It has been reported that lysine 118 (K118) represents a major SUMOylation site on AMPKα, and mutating the 118th lysine residue to arginine blocked AMPKα SUMOylation (25). We therefore generated the mutated (K118R) AMPKα and found that the SUMOylation of mutated AMPKα was decreased as compared with WT AMPKα (Fig. 6*G*). DeSUMOylated AMPKα (K118R) exhibited shortened half-life as compared with WT AMPKα (Fig. 6*H*), which was consistent with the observation that SENP2 repressed AMPKα level. Taken together, our data suggest that SENP2 induces AMPKα ubiquitination and sequential degradation, likely through the deSUMOylation of AMPKα.

Discussion

Based on the present findings, we propose a potential mechanism by which hepatic SENP2 regulates gluconeogenesis. We hypothesize that SENP2 is responsible for catalyzing the deSUMOylation of AMPKα, leading to ubiquitylation and subsequent degradation of AMPKα, and resulting in augmented gluconeogenesis (Fig. 7). We found that overexpression of SENP2 promoted gluconeogenesis and increased blood glucose levels, whereas hepatic gluconeogenesis was dramatically downregulated in SENP2-deficient hepatocytes. As a result, Senp2-LKO mice were resistant to HFD-induced hyperglycemia. Inhibition of AMPKα by siRNA or inhibitor restored gluconeogenesis in Senp2-LKO mice.

We previously reported that SENP2 was significantly increased in the liver of HFD-induced T2D mice (23), which supported the notion that SENP2 promotes gluconeogenesis. Previous studies have reported that SENP2 is induced upon activation of the cAMP–PKA–CREB axis in adipocytes (19) and that SENP2 expression is regulated by palmitate-induced NF-κB activation in skeletal muscle (22). Although we did not directly access the factors that regulate SENP2 expression in the liver, specific metabolites and hormones associated with HFD feeding such as glucagon and glucocorticoid may be involved.

Hepatic gluconeogenesis is controlled by the transcriptional regulation of key rate-limiting enzymes. At present, most studies on gluconeogenesis have focused on the expression and regulation of the gluconeogenic enzymes PCK1 and G6PC. Interestingly, in the current study, we demonstrated that expression of the gluconeogenic enzyme PCx was significantly decreased by SENP2 disruption, whereas other enzymes such as PCK1 and G6PC were unaffected. PCx catalyzes the first step of gluconeogenesis and is therefore critical for maintaining glucose metabolic homeostasis (26, 27). Kumashiro *et al.* (26) measured the mRNA and protein expression of key gluconeogenic enzymes in human liver specimens and found that only hepatic PCx protein levels correlated strongly with glycemia. Inhibition of PCx reduced plasma glucose concentrations and the rate of endogenous glucose production *in vivo* (26). Here, we found that SENP2 regulated PCx expression *via* AMPKα. However, it remains unclear why SENP2 solely modulated PCx but not PCK1 and G6PC. Furthermore, although compound C or siAMPKα completely reversed the decrease in PCx levels induced by SENP2 deficiency in cellular model, they only partially rescued PCx protein levels *in vivo*,

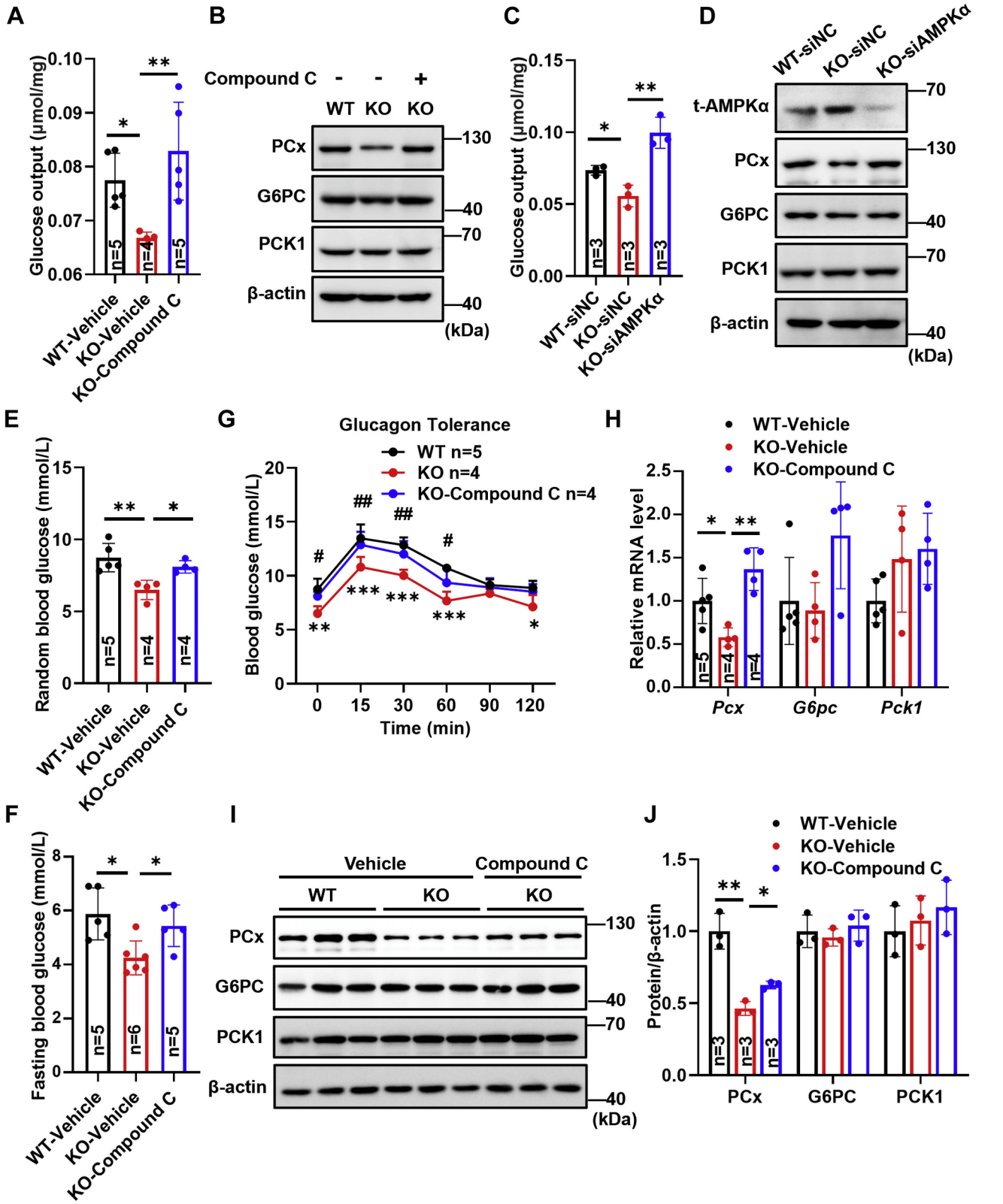

Figure 5. Inhibition of AMPK reversed the decreased blood glucose and hepatic gluconeogenesis in Senp2-LKO mice. *A* and *B*, primary hepatocytes were isolated from WT and Senp2-LKO mice under NCD and were treated with compound C (5 μm) to inhibit AMPK. Glucose output of the isolated hepatocytes with dexamethasone treatment was detected (*A*). Western blot analysis of PCx, G6PC, and PCK1 in the isolated hepatocytes (*B*). *C* and *D*, primary hepatocytes were isolated from WT and Senp2-LKO mice. AMPKα was disrupted by siAMPKα. Glucose output of the isolated hepatocytes was then detected (*C*). Western blot analysis of PCx, G6PC, and PCK1 in the isolated hepatocytes (*D*). *E–J*, WT and Senp2-LKO mice were fed with HFD for 12 weeks and then intraperitoneally injected with compound C (20 mg/kg) for 5 days to inhibit AMPK. *E* and *F*, random and fasting blood glucose levels were measured at 13th week of HFD feeding. *G*, glucagon tolerance test was then performed at 13th week of HFD feeding. *H*, qPCR analysis of mRNA level of *PCx*, *G6PC*, and *PCK1* in the liver. *I* and *J*, Western blot analysis of PCx, G6PC, and PCK1 in the liver. Data are presented as mean ± SD. Data in *A*, *C*, *E*, *F*, *H*,

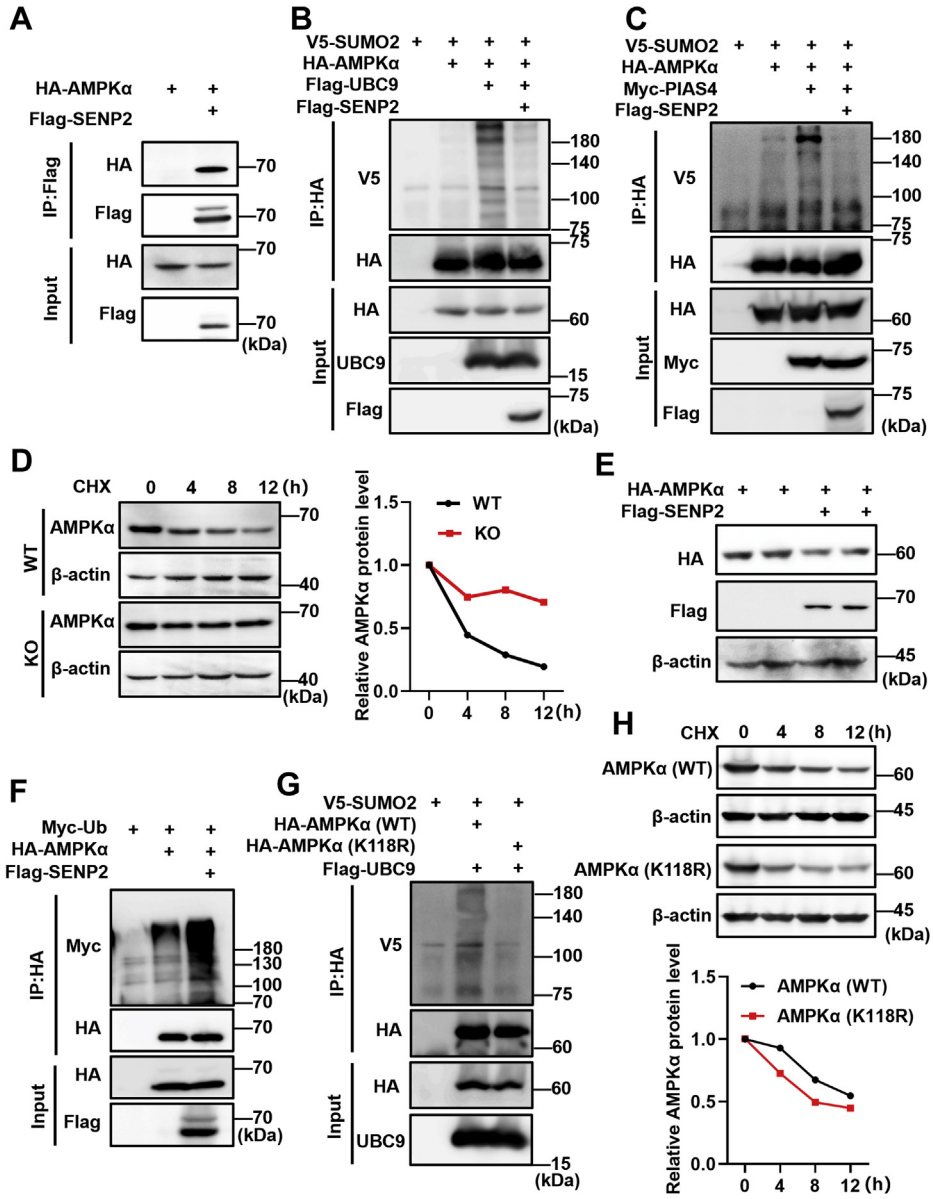

Figure 6. SENP2 deSUMOylated AMPKα and promoted its ubiquitylation and degradation. *A*, co-IP was conducted in the HEK-293T cells using antibody against FLAG tag. *B*, the vectors harboring V5-SUMO2, HA-AMPKα, FLAG-UBC9, and FLAG-SENP2 were transfected into HEK-293T cells as indicated. At 36th h after transfection, IP was conducted by HA tag. AMPKα SUMOylation was detected by Western blot using V5 antibody. *C*, the vectors harboring V5-SUMO2, HA-AMPKα, Myc-PIAS4, and FLAG-SENP2 were transfected into HEK-293T cells as indicated. At 36th h after transfection, IP was conducted by HA tag. AMPKα SUMOylation was detected by Western blot using V5 antibody. *D*, primary hepatocytes isolated from WT or Senp2-LKO mice were treated with 10 μM cycloheximide (CHX) for 0, 4, 8, and 12 h, and AMPKα was detected by Western blot. *E*, SENP2 was overexpressed in HEK-293T cells and then subjected to detection of AMPKα expression. *F*, the indicated vectors were transfected into HEK-293T cells. At 36th h after transfection, cells were harvested after MG132 incubation, and IP was conducted by HA tag. AMPKα ubiquitylation was detected by Western blot using Myc antibody. *G*, WT AMPKα or AMPKα (K118R) was transfected into HEK-293T cells. At 36th h after transfection, IP was conducted by HA tag. AMPKα SUMOylation was detected by Western blot using V5 antibody. *H*, WT AMPKα or AMPKα (K118R) was transfected into HEK-293T cells. At 36th h after transfection, cells were treated with 10 μM CHX for 0, 4, 8, and 12 h and then for AMPKα detection. AMPK, 5′-AMP-activated protein kinase; co-IP, coimmunoprecipitation; HA, hemagglutinin; HEK-293T, human embryonic kidney 293T cell; SENP2, small ubiquitin–related modifier–specific protease 2.

suggesting that other AMPKα targets might be involved in the regulation of gluconeogenesis.

Although AMPKα has an important physiological function in the regulation of biological energy homeostasis, its role in gluconeogenesis is controversial. Some evidence has demonstrated that hepatic AMPK deficiency has little effect on gluconeogenesis and specifically does not impact the effects of metformin on gluconeogenesis (28, 29). In contrast, other

and *J* were analyzed by using one-way ANOVA with Newman–Keuls test. $^{*}p < 0.05$, $^{**}p < 0.01$, $^{***}p < 0.001$. Data in *G* were analyzed by two-way ANOVA with Bonferroni post hoc multiple comparison test. $^{*}p < 0.05$, $^{**}p < 0.01$, and $^{***}p < 0.001$ compared between WT and KO mice; $^{\#}p < 0.05$; $^{\#\#}p < 0.01$; and $^{\#\#\#}p < 0.001$ compared between KO and KO-compound C mice. AMPK, 5′-AMP-activated protein kinase; G6PC, glucose-6-phosphatase; LKO, liver-specific knockout mice; NCD, normal chow diet; PCK1, phosphoenolpyruvate carboxykinase 1; PCx, pyruvate carboxylase; qPCR, quantitative PCR.

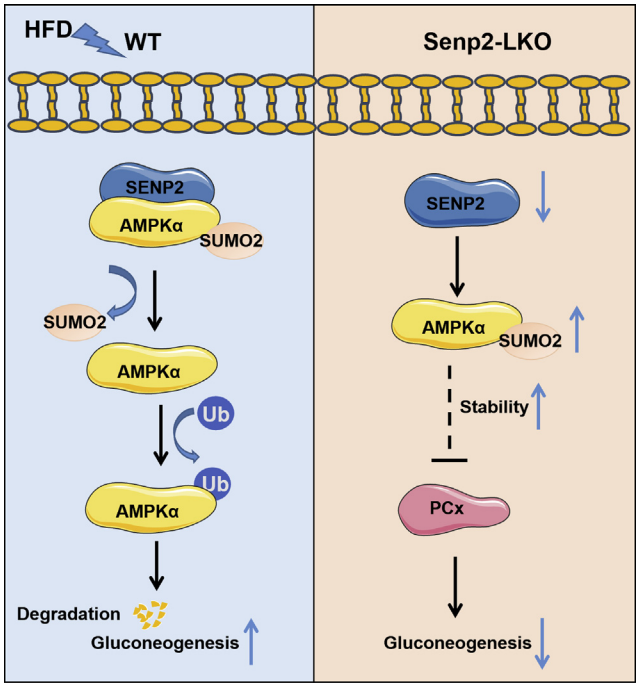

Figure 7. Model of the role of SENP2 in regulating hepatic gluconeogenesis. SENP2 was responsible for catalyzing the deSUMOylation of AMPKα, leading to ubiquitylation and subsequent degradation of AMPKα, and resulting in augmented gluconeogenesis. Overexpression of SENP2 promoted gluconeogenesis and increased blood glucose levels. In SENP2-deficient hepatocytes, SUMOylation of AMPKα was increased, which promoted its stability and then inhibited gluconeogenesis. As a result, Senp2-LKO mice were resistant to HFD-induced hyperglycemia. AMPK, 5′-AMP-activated protein kinase; HFD, high-fat diet; LKO, liver-specific knockout mice; SENP2, small ubiquitin–related modifier–specific protease 2.

studies have shown that activation of AMPK or overexpression of constitutively active AMPK dramatically inhibits hepatic gluconeogenesis (12, 13, 30). Here, we observed a significant increase in AMPKα protein expression in liver tissue and primary hepatocytes of Senp2-LKO mice. Inhibition of AMPKα by siRNA or inhibitor completely restored gluconeogenesis in Senp2-LKO mice. These findings suggest that AMPK may negatively regulate hepatic gluconeogenesis.

We also demonstrated that SENP2 could interact with AMPKα and deSUMOylate it. Previous studies have reported that AMPK subunits can be SUMOylated. For example, PIAS4 catalyzed the SUMOylation of AMPKα (25), whereas SUMOylation of AMPKα1 attenuated AMPK activation and specifically activated mammalian target of rapamycin complex 1 signaling (25). In contrast, SUMOylation of AMPKβ2 by PIASy enhanced the activity of the trimeric α2β2γ1 AMPK complex (31). AMPKβ2 SUMOylation is antagonistic and competes with ubiquitination of the AMPKβ2 subunit (31). Here, we found that SUMOylation affected AMPK protein stability. The dramatic increase in AMPKα protein levels in the liver of Senp2-LKO mice was associated with an increase in the activated form as measured by phosphorylation of AMPKα-T172. We mutated K118 residue of AMPKα, which was considered as the major SUMOylated site, and found that SUMOylation level of AMPKα (K118R) was decreased (Fig. 6*G*), though K118 might not be the unique modified site of SUMO2 according to our data. Notably, AMPKα (K118R) was less stable than WT (Fig. 6*H*), which was consistent with the noting that SENP2 deSUMOylated AMPKα and reduced its stability. Although the precise underlying mechanisms mediating the transition between AMPKα SUMOylation and ubiquitylation remain unclear, we hypothesize that it may involve an association between AMPKα and its E3 ubiquitin ligase. Thus, future studies should focus on examining the interaction between E3 ubiquitin ligase and SUMOylated or unSUMOylated AMPK. In summary, the current study describes a novel SENP2–AMPKα axis that links SUMOylation to regulation of gluconeogenesis and suggests that the SENP2–AMPKα axis may be a potential target for clinical interventions of T2D.

Experimental procedures

Animal study

$SENP2^{Flox/flox}$ mice were provided by Dr Cheng (Shanghai Jiao Tong University School of Medicine) and generated as described previously (32). $SENP2^{Flox/flox}$ mice were bred with Alb-Cre mice to obtain specific SENP2 knockout mice in liver tissue. The genotype of the knockout mice was $SENP2^{Flox/flox}$ and Alb-Cre positive. WT mice were selected as control mice with the genotype of $SENP2^{Flox/flox}$ and Alb-Cre negative. PCR amplification analysis showed that 149 bp were negative, 149 bp and 183 bp were heterozygous, and 183 bp were positive. The following primers were used: Flox forward primer: CTTCTGCTTCTCTTAGTGCT; Flox reverse primer: AAGAGCAAGCACTCTTACTG; Alb-Cre forward primer: TTGGCCCCTTACCATAACTG; and Alb-Cre reverse primer: GAAG CAGAAGCTTAGGAAGATGG.

All the mice were housed at room temperature (25 °C), with a 12-h light–dark cycle and *ad libitum* access to NCD (70% kcal from carbohydrate, 20% kcal from protein, and 10% kcal from fat) and water. For diet challenge, male mice were fed with an HFD (60% kcal from fat, 20% kcal from protein, and 20% kcal from carbohydrate; D12492; Research Diets, Inc) starting at 8 weeks of age. All studies involving animal experimentation were approved by the Fudan University Shanghai Medical College Animal Care and Use Committee and followed the National Institutes of Health guidelines on the care and use of animals.

For SENP2 overexpression in the liver, AAV serotype 8 harboring the SENP2 coding sequence and the control were purchased from Hanbio Tech (Shanghai) Co, Ltd. AAVs were injected into 7-week-old male mice *via* the tail vein. After a week of recovery, AAV-treated mice were fed with HFD and then subjected to metabolic measurements.

Preparation of mouse primary hepatocytes

The mice fed with NCD were anesthetized, and their abdominal hair was cleaned. An infusion tube was inserted into the hepatic portal vein and fixed with a hemostatic clip. Liver tissues were washed with sterile calcium- and magnesium-free Hank's balanced salt solution buffer (138 mM NaCl, 5.4 mM KCl, 0.3 mM Na_2HPO_4, 0.4 mM KH_2PO_4,

5.6 mM glucose, 0.5 mM EGTA, and 4 mM $NaHCO_3$), and 0.04% collagenase prepared with Hank's balanced salt solution buffer (138 mM NaCl, 5.4 mM KCl, 0.3 mM Na_2HPO_4, 0.4 mM KH_2PO_4, 5.6 mM glucose, 0.8 mM $MgSO_4$, 1.26 mM $CaCl_2{\cdot}2H_2O$, and 4 mM $NaHCO_3$) was used for digestion. After digestion, the liver tissue was removed and shaken to loosen the hepatocytes, and the tissue fragments were filtered through a 100 μm cell sieve. Primary hepatocytes were then collected by centrifugation, purified with Percoll solution, counted, and plated.

siRNA transfection

After isolation of primary hepatocytes from mice, the cells were seeded into 12-well plates and transfected with siRNA. Briefly, 50 μl Opti-minimal essential medium (MEM) containing 1.5 pmol siRNA and 50 μl opti-MEM containing 1.5 μl RNA iMAX transfection reagent were gently mixed and left for 20 min. At the same time, the cell supernatant was removed, and 1 ml opti-MEM was replaced. The siRNA mixture was added slowly to the cells, and the culture plate was shaken gently. After 12 to 24 h, the transfection medium was replaced with normal culture medium, and subsequent experiments were performed 48 h after transfection. The following sequences for siRNA were used: siNC, UUCUUCGAACGUGUCACGUTT and ACGUGACACGUUCGGAGAATT; and siAMPKα, CAUCUUAUAGUUCAACCAUTT and AUGGUUGAACUAUAAGAUGGG.

Pyruvate tolerance test

Gluconeogenesis activity was measured by performing the pyruvate tolerance test. Briefly, mice in each group were starved overnight. After the initial fasting, blood glucose levels were measured, and the mice were injected with sodium pyruvate solution (20% sodium pyruvate dissolved in normal saline) intraperitoneally at a dose of 2 g/kg body weight. Blood glucose levels were measured at different time points.

Glucagon tolerance test

The glucagon tolerance test was used to evaluate gluconeogenesis. Mice were starved for 4 to 6 h and then injected with glucagon intraperitoneally at a dose of 10 μg/kg. Blood glucose levels were measured in blood samples taken from the tail vein at the indicated postinjection time points.

Glucose production in primary hepatocytes

Cells were washed 3 to 4 times with PBS and incubated with glucose substrate solution containing 10 mM sodium lactate, 1 mM sodium pyruvate, with or without 1 μM dexamethasone. The cell media were collected after incubation for 6 h. After centrifugation, the glucose content in the cell media was detected using a glucose detection kit (APPLYGEN). Glucose level was normalized to the total protein level.

RT–PCR and real-time quantitative PCR

RNA was extracted from cells or tissues with Trizol reagent and dissolved in diethyl pyrocarbonate water. The RNA (500 ng) was reverse transcribed using the TaKaRa Reverse Transcription Kit (TaKaRa Bio). Using a ChamQ Universal SYBR qPCR Master Mix (Vazyme) and complementary DNA as the template, the target fragment was amplified by adding specific primers of the gene of interest, and the expression level of the gene of interest was reflected by the fluorescence intensity of the target fragment. Each reaction was performed in triplicate. Relative mRNA levels were calculated according to the Ct value, and the Ct value of 18s rRNA was used for normalization. The following forward and reverse primers (5′ to 3′) were used for RT–PCR: *Senp2*, AAGAACAGTCTCTACAATGCTGC and CCGATTTCAGCGTAAAACCAAAG; *Pcx*, GATGACCTCACAGCCAAGCA and GGGTACCTCTGTGTCCAAAGGA; *Pck1*, CTGCATAACGGTCTGGACTTC and CAGCAACTGCCCGTACTCC; *G6pc*, CGACTCGCTATCTCCAAGTGA and GTTGAACCAGTCTCCGACCA; and *Ampkα*, GTCAAAGCCGACCCAATGATA and CGTACACGCAAATAATAGGGGTT.

Western blotting

Tissues or cells were lysed and then denatured at 100 °C for 10 min. The protein concentration was determined by bicinchoninic acid assay. Equal amounts of protein were separated by SDS-PAGE, transferred to a polyvinylidene difluoride membrane (Millipore Corp), and immunoblotted with the following primary antibodies: SENP2 (YT4237) was from Immunoway; phospho-AMPKα (2535S), AMPKα (5832S), phosphor-Raptor (2083), Raptor (2280), and HA tag (3724) were from Cell Signaling Technology; G6PC (A16234) and PCK1 (A2036) were from Abclonal; FLAG tag (F1804) and β-actin (A5441) were from Sigma–Aldrich; Myc tag (E022050-02) was from EARTH, and PCx (16588-1-AP) was from Proteintech. The specificity and reproducibility of the used antibodies were validated.

Coimmunoprecipitation

HEK-293T cells transfected with HA-AMPKα or FLAG-SENP2 were lysed in lysis buffer containing 50 mM Tris–Hcl (pH 7.5), 150 mM NaCl, 5% glycerol, 0.5% Triton X-100, and protease inhibitors (Roche). After centrifugation, the lysates were incubated with anti-FLAG beads (SMART LIFESCIENCES) for 2 h. The beads were then washed four times with washing buffer (50 mM Tris–Hcl [pH 7.5], 100 mM NaCl, 5% glycerol, 0.1% Triton X-100, and protease inhibitors), and the immunoprecipitates were separated by SDS-PAGE for Western blotting.

SUMO modification experiment

The V5-SUMO plasmid, HA-AMPKα plasmid, FLAG-SENP2 plasmid, and FLAG-UBC9 plasmid were transfected into HEK-293T cells. HEK-293T cells were lysed in lysis buffer containing 50 mM Tris–Hcl (pH 8.0), 250 mM NaCl, 0.01% Tween, 1% Triton X-100, 0.0125 g/ml *N*-ethylmaleimide, and protease inhibitors (Roche). After centrifugation, lysates were incubated with anti-HA beads (SMART LIFESCIENCES) and rotated at 4 °C for 2 h. The beads were then washed four times

with washing buffer (50 mM Tris–Hcl [pH 8.0], 250 mM NaCl, 0.01% Tween, 0.0125 g/ml *N*-ethylmaleimide, and protease inhibitors). Finally, the immunocoprecipitates were subjected to Western blotting using V5 antibody to detect SUMOylated AMPKα.

Ubiquitin modification experiment

HEK-293T cells were transfected with HA-AMPKα plasmid, FLAG-SENP2 plasmid, and Myc-Ub plasmid. After 36 h of transfection, cells were treated with 10 μM proteasome inhibitor MG132 for 4 to 5 h, and ubiquitination was detected. Briefly, transfected cells were lysed in Ub lysate buffer containing 50 mM Tris–HCl (pH 8.0), 150 mM NaCl, 1% NP-40, 1% SDS, and protease inhibitors (Roche). Cell lysates were boiled for 10 min at 100 °C to denature the protein. After centrifugation for 10 min, the supernatant was diluted 10-fold in dilution buffer (50 mM Tris–HCl [pH 8.0] and 150 mM NaCl) and added to anti-HA beads (SMART LIFESCIENCES). After rotation at 4 °C for 2 h, the agarose beads were washed four times. Finally, the immunocoprecipitates were detected by Western blotting.

Statistical analysis

GraphPad software (GraphPad Software, Inc) was used for statistical analysis. All data were presented as mean ± SD with statistical significance. Two-tailed unpaired Student's *t* test was used to compare two groups with normally distributed data. One-way ANOVA was used to compare more than two groups. Two-way ANOVA with Bonferroni post hoc multiple comparison test was used to analyze assays such as the glucagon tolerance and pyruvate tolerance tests. $p < 0.05$ was considered to be of statistical significance. The statistical analysis used in each panel is described in the legends to the figures.

Data availability

All data are contained within the article.

Supporting information—This article contains supporting information.

Acknowledgments—We are grateful to Dr Cheng J.K. (Shanghai Jiao Tong University School of Medicine) for providing SENP2$^{Flox/flox}$ mice.

Author contributions—Y. L., Q.-Q. T., Q.-Q. Y., S.-W. Q., and Y. T. conceptualization; X. D., W.-Y. Z., M. D., and Y.-J. M. investigation; X. D. and Y. L. data curation; X. D., Q.-Q. T., and Y. L. writing–reviewing and editing; Q.-Q. T. and Y. L. supervision; Q.-Q. T. and Y. L. funding acquisition.

Funding and additional information—This work was supported by the National Key R&D Program of China (grant number: 2018YFA0800400 [to Q.-Q. T.]), National Natural Science Foundation of China grants (grant numbers: 81970744 [to Y. L.] and 81730021 [to Q.-Q. T.]), Scientific research projects of Shanghai Health Commission (grant number: 20204Y0116), China Postdoctoral Science Foundation grant (grant numbers: 2016M600282 and 2017T100268; to Y. L.), and Science and Technology Development Fund of Shanghai Pudong New Area (grant no.: PKJ2020-Y48).

Conflict of interest—The authors declare that they have no conflicts of interest with the contents of this article.

Abbreviations—The abbreviations used are: AAV, adeno-associated virus; AMPK, 5′-AMP-activated protein kinase; CREB, cAMP response element–binding protein; G6PC, glucose-6-phosphatase; HA, hemagglutinin; HEK-293T, human embryonic kidney 293T cell; HFD, high-fat diet; K118, lysine 118; LKO, liver-specific knockout mice; MEM, minimal essential medium; NCD, normal chow diet; PCK1, phosphoenolpyruvate carboxykinase 1; PCx, pyruvate carboxylase; PIAS, protein inhibitor of activated signal transducer and activator of transcription; qPCR, quantitative PCR; SENP2, small ubiquitin–related modifier–specific protease 2; SUMO, small ubiquitin–related modifier; T2D, type 2 diabetes; TORC2, transducer of regulated CREB activity 2.

References

1. Petersen, M. C., Vatner, D. F., and Shulman, G. I. (2017) Regulation of hepatic glucose metabolism in health and disease. *Nat. Rev. Endocrinol.* **13**, 572–587
2. Landau, B. R., Wahren, J., Chandramouli, V., Schumann, W. C., Ekberg, K., and Kalhan, S. C. (1996) Contributions of gluconeogenesis to glucose production in the fasted state. *J. Clin. Invest.* **98**, 378–385
3. Zechner, R., Madeo, F., and Kratky, D. (2017) Cytosolic lipolysis and lipophagy: Two sides of the same coin. *Nat. Rev. Mol. Cell Biol.* **18**, 671–684
4. Nurjhan, N., Consoli, A., and Gerich, J. (1992) Increased lipolysis and its consequences on gluconeogenesis in non-insulin-dependent diabetes mellitus. *J. Clin. Invest.* **89**, 169–175
5. Sargsyan, A., and Herman, M. A. (2019) Regulation of glucose production in the pathogenesis of type 2 diabetes. *Curr. Diab. Rep.* **19**, 77
6. Magnusson, I., Rothman, D. L., Katz, L. D., Shulman, R. G., and Shulman, G. I. (1992) Increased rate of gluconeogenesis in type II diabetes mellitus. A 13C nuclear magnetic resonance study. *J. Clin. Invest.* **90**, 1323–1327
7. Gonzalez, A., Hall, M. N., Lin, S. C., and Hardie, D. G. (2020) AMPK and TOR: The Yin and Yang of cellular nutrient sensing and growth control. *Cell Metab.* **31**, 472–492
8. Hardie, D. G., Ross, F. A., and Hawley, S. A. (2012) AMPK: A nutrient and energy sensor that maintains energy homeostasis. *Nat. Rev. Mol. Cell Biol.* **13**, 251–262
9. Ross, F. A., MacKintosh, C., and Hardie, D. G. (2016) AMP-activated protein kinase: A cellular energy sensor that comes in 12 flavours. *FEBS J.* **283**, 2987–3001
10. Hawley, S. A., Boudeau, J., Reid, J. L., Mustard, K. J., Udd, L., Makela, T. P., Alessi, D. R., and Hardie, D. G. (2003) Complexes between the LKB1 tumor suppressor, STRAD alpha/beta and MO25 alpha/beta are upstream kinases in the AMP-activated protein kinase cascade. *J. Biol.* **2**, 28
11. Woods, A., Johnstone, S. R., Dickerson, K., Leiper, F. C., Fryer, L. G., Neumann, D., Schlattner, U., Wallimann, T., Carlson, M., and Carling, D. (2003) LKB1 is the upstream kinase in the AMP-activated protein kinase cascade. *Curr. Biol.* **13**, 2004–2008
12. Koo, S. H., Flechner, L., Qi, L., Zhang, X., Screaton, R. A., Jeffries, S., Hedrick, S., Xu, W., Boussouar, F., Brindle, P., Takemori, H., and Montminy, M. (2005) The CREB coactivator TORC2 is a key regulator of fasting glucose metabolism. *Nature* **437**, 1109–1111
13. Lee, J. M., Seo, W. Y., Song, K. H., Chanda, D., Kim, Y. D., Kim, D. K., Lee, M. W., Ryu, D., Kim, Y. H., Noh, J. R., Lee, C. H., Chiang, J. Y., Koo, S. H., and Choi, H. S. (2010) AMPK-dependent repression of hepatic gluconeogenesis via disruption of CREB.CRTC2 complex by orphan nuclear receptor small heterodimer partner. *J. Biol. Chem.* **285**, 32182–32191

14. Celen, A. B., and Sahin, U. (2020) Sumoylation on its 25th anniversary: Mechanisms, pathology, and emerging concepts. *FEBS J.* **287**, 3110–3140
15. Flotho, A., and Melchior, F. (2013) Sumoylation: A regulatory protein modification in health and disease. *Annu. Rev. Biochem.* **82**, 357–385
16. Liu, Y., Zhang, Y. D., Guo, L., Huang, H. Y., Zhu, H., Huang, J. X., Liu, Y., Zhou, S. R., Dang, Y. J., Li, X., and Tang, Q. Q. (2013) Protein inhibitor of activated STAT 1 (PIAS1) is identified as the SUMO E3 ligase of CCAAT/enhancer-binding protein beta (C/EBPbeta) during adipogenesis. *Mol. Cell. Biol.* **33**, 4606–4617
17. Liu, Y., Ge, X., Dou, X., Guo, L., Liu, Y., Zhou, S. R., Wei, X. B., Qian, S. W., Huang, H. Y., Xu, C. J., Jia, W. P., Dang, Y. J., Li, X., and Tang, Q. Q. (2015) Protein inhibitor of activated STAT 1 (PIAS1) protects against obesity-induced insulin resistance by inhibiting inflammation cascade in adipose tissue. *Diabetes* **64**, 4061–4074
18. Kunz, K., Piller, T., and Muller, S. (2018) SUMO-specific proteases and isopeptidases of the SENP family at a glance. *J. Cell Sci.* **131**, jcs211904
19. Chung, S. S., Ahn, B. Y., Kim, M., Choi, H. H., Park, H. S., Kang, S., Park, S. G., Kim, Y. B., Cho, Y. M., Lee, H. K., Chung, C. H., and Park, K. S. (2010) Control of adipogenesis by the SUMO-specific protease SENP2. *Mol. Cell. Biol.* **30**, 2135–2146
20. Liang, Q., Zheng, Q., Zuo, Y., Chen, Y., Ma, J., Ni, P., and Cheng, J. (2019) SENP2 suppresses necdin expression to promote brown adipocyte differentiation. *Cell Rep.* **28**, 2004–2011.e4
21. Zheng, Q., Cao, Y., Chen, Y., Wang, J., Fan, Q., Huang, X., Wang, Y., Wang, T., Wang, X., Ma, J., and Cheng, J. (2018) Senp2 regulates adipose lipid storage by de-SUMOylation of Setdb1. *J. Mol. Cell. Biol.* **10**, 258–266
22. Koo, Y. D., Choi, J. W., Kim, M., Chae, S., Ahn, B. Y., Kim, M., Oh, B. C., Hwang, D., Seol, J. H., Kim, Y. B., Park, Y. J., Chung, S. S., and Park, K. S. (2015) SUMO-specific protease 2 (SENP2) is an important regulator of fatty acid metabolism in skeletal muscle. *Diabetes* **64**, 2420–2431
23. Liu, Y., Dou, X., Zhou, W. Y., Ding, M., Liu, L., Du, R. Q., Guo, L., Qian, S. W., Tang, Y., Yang, Q. Q., Pan, D. N., Li, X. Y., Lu, Y., Cheng, J. K., and Tang, Q. Q. (2021) Hepatic small ubiquitin-related modifier (SUMO)-specific protease 2 controls systemic metabolism through SUMOylation-dependent regulation of liver-adipose tissue crosstalk. *Hepatology* **74**, 1864–1883
24. Carling, D. (2017) AMPK signalling in health and disease. *Curr. Opin. Cell Biol.* **45**, 31–37
25. Yan, Y., Ollila, S., Wong, I. P. L., Vallenius, T., Palvimo, J. J., Vaahtomeri, K., and Makela, T. P. (2015) SUMOylation of AMPKalpha1 by PIAS4 specifically regulates mTORC1 signalling. *Nat. Commun.* **6**, 8979
26. Kumashiro, N., Beddow, S. A., Vatner, D. F., Majumdar, S. K., Cantley, J. L., Guebre-Egziabher, F., Fat, I., Guigni, B., Jurczak, M. J., Birkenfeld, A. L., Kahn, M., Perler, B. K., Puchowicz, M. A., Manchem, V. P., Bhanot, S., *et al.* (2013) Targeting pyruvate carboxylase reduces gluconeogenesis and adiposity and improves insulin resistance. *Diabetes* **62**, 2183–2194
27. Pereira, R. M., Rodrigues, K., Sant'Ana, M. R., Peruca, G. F., Morelli, A. P., Simabuco, F. M., da Silva, A. S. R., Cintra, D. E., Ropelle, E. R., Pauli, J. R., and de Moura, L. P. (2020) Strength exercise reduces hepatic pyruvate carboxylase and gluconeogenesis in DIO mice. *J. Endocrinol.* **247**, 127–138
28. Foretz, M., Hebrard, S., Leclerc, J., Zarrinpashneh, E., Soty, M., Mithieux, G., Sakamoto, K., Andreelli, F., and Viollet, B. (2010) Metformin inhibits hepatic gluconeogenesis in mice independently of the LKB1/AMPK pathway via a decrease in hepatic energy state. *J. Clin. Invest.* **120**, 2355–2369
29. Hasenour, C. M., Ridley, D. E., James, F. D., Hughey, C. C., Donahue, E. P., Viollet, B., Foretz, M., Young, J. D., and Wasserman, D. H. (2017) Liver AMP-activated protein kinase is unnecessary for gluconeogenesis but protects energy state during nutrient deprivation. *PLoS One* **12**, e0170382
30. Woods, A., Williams, J. R., Muckett, P. J., Mayer, F. V., Liljevald, M., Bohlooly, Y. M., and Carling, D. (2017) Liver-specific activation of AMPK prevents steatosis on a high-fructose diet. *Cell Rep.* **18**, 3043–3051
31. Rubio, T., Vernia, S., and Sanz, P. (2013) Sumoylation of AMPKbeta2 subunit enhances AMP-activated protein kinase activity. *Mol. Biol. Cell* **24**, 1801–1811. S1–4
32. Qi, Y., Wang, J., Bomben, V. C., Li, D. P., Chen, S. R., Sun, H., Xi, Y., Reed, J. G., Cheng, J., Pan, H. L., Noebels, J. L., and Yeh, E. T. (2014) Hyper-SUMOylation of the Kv7 potassium channel diminishes the M-current leading to seizures and sudden death. *Neuron* **83**, 1159–1171